Laser-induced chemical vapor deposition of hydrogenated amorphous silicon. II. Film properties

M. Meunier,[a] J. H. Flint, J. S. Haggerty, and D. Adler[b]
Massachusetts Institute of Technology, Cambridge, Massachusetts 02139

(Received 17 March 1987; accepted for publication 9 June 1987)

Properties of hydrogenated amorphous silicon thin films prepared by the laser-induced chemical vapor deposition (LICVD) of silane gas are described. We report the results of measurements of hydrogen concentration, infrared absorption, unpaired-spin density, optical and mechanical properties, electrical conductivity, and photoconductivity experiments. We conclude that the film properties are controlled primarily by the substrate temperature T_s. LICVD films are superior to those produced by conventional CVD because of the permissibly low values of T_s. This results in an increased hydrogen content (up to 30 at. %) and a reduced defect density ($\sim 10^{16}$ spins/cm^3). The hydrogen concentration is determined by the surface chemistry for $T_s < 300$ °C ([H] > 20 at. %) and by H_2 evolution for $T_s > 300$ °C([H] < 20 at. %). The hydrogen is incorporated primarily in the SiH_2 configuration and for $T_s < 300$ °C, the films contain some polysilane $(SiH_2)_n$ regions. All the physical properties of the films are discussed in conjunction with the LICVD process characteristics and are also compared with the properties of films prepared by the plasma-decomposition and homogeneous chemical vapor deposition (HOMOCVD) techniques. In all cases, the differences can be attributed to variations in the processing conditions.

I. INTRODUCTION

Recent interest in hydrogenated amorphous silicon (*a*-Si:H) films has been spurred by its technological promise as an inexpensive material for use in large-area solar energy-conversion devices,[1] thin-film transistors,[2] image sensors,[3] charge-coupled devices,[4] electrophotography,[5] and vidicon devices.[6] Each of these applications demands specific, but widely different structural, electrical, and optical properties for the active *a*-Si:H layers. However, all of these properties depend on the nature and concentration of the various types of defects which, in turn are directly influenced by the preparation method. Therefore, it is of great importance to find an appropriate processing method which minimizes the overall defect concentration. With this in mind, we have investigated the properties of *a*-Si:H prepared by the relatively new process, laser-induced chemical vapor deposition (LICVD).

The LICVD technique was developed independently and concurrently by Bilenchi, Gianinoni, and Musci[7] and by Gattuso *et al.*[8,9] A process model is proposed in the previous paper.[10] Very briefly, we used a CO_2 laser on the $P(20)$ line, 10.591 μm, to heat up a gas mixture, which includes SiH_4, and thus thermally decomposes the SiH_4. The laser is aligned parallel to the substrate upon which the film is to be deposited, allowing independent control of both the gas and substrate temperatures. Due to the high directionality of the laser, the walls of the reactor are cold eliminating contamination from the walls, a major problem of hot-wall reactors. For example, in a glow-discharge process, the interaction between the reactor walls and the plasma may cause impurities to be incorporated into the growing film. Moreover, the plasma contains various highly energetic ionic species which can lead to the introduction of defects upon bombardment of the film surface.[11,12] However, LICVD is a cold-wall thermal process, in which the growth environment contains no high-energy particles and very limited impurity concentrations. We have proposed a process model,[10] in which the *a*-Si:H thin-film growth is rate controlled by the gas-phase homogeneous thermal decomposition of SiH_4. Similar to the HOMOCVD process,[12,13] the gas-phase chemistry involves the production of SiH_2 and higher diradicals resulting from the pyrolysis of SiH_4. These diradicals diffuse out of the laser beam to the substrate leading to the growth of *a*-Si:H films.

In order to evaluate the quality of the films deposited by LICVD, we must thoroughly characterize the material. This involves investigations of the structure and composition, the spin density, and the mechanical, optical, and electrical properties of the films. As expected, we find that most of these properties are primarily controlled by the substrate temperature. Indeed, the film properties are superior to those of *a*-Si prepared by conventional CVD and are quite similar to those produced by glow discharge and HOMOCVD. They reflect the qualities that might be anticipated for this deposition technique; the permissibly low substrate temperatures directly lead to increased hydrogen concentrations relative to conventional CVD films, and concomitantly the material exhibits drastically reduced defect densities.

In the following sections, we present and discuss the properties of the films in relation to the specific characteristics of the LICVD process. We also describe a growth process in which the composition and structure of the material depend on the competition between the surface chemistry

[a] Present address: Department of Engineering Physics, and Groupe des Couches Minces, Ecole Polytechnique de Montreal, Montreal, Quebec, Canada H3C 3A7.

[b] Professor David Adler died suddenly on March 31, 1987. We will long remember his precise thinking and his vast culture, and most importantly his friendship for his collaborators.

 0021-8979/87/192822-08$02.40 © 1987 American Institute of Physics

and the H_2 evolution process. All the properties seem to be in accord with this growth process. The characteristics of LICVD films are also compared with those of films made by plasma and HOMOCVD techniques and differences are related to the different processing conditions.

II. COMPOSITION AND STRUCTURE OF LICVD FILMS

Depending on the particular measurement to be performed, films were deposited on a variety of substrates, including borosilicate glass (Corning 0211), aluminum-coated glass, fused silica, and single-crystal silicon. All films were determined to be amorphous from the results of electron-diffraction experiments, as expected with the low substrate temperatures used ($T_s < 400$ °C). The film composition was investigated both by the H_2 effusion technique[14] and by infrared (IR) spectroscopy.[15–17]

Figure 1 shows the H content, [H], as a function of T_s for both our LICVD films and conventional CVD films.[18] [H] was determined by the effusion technique[14] for films deposited on fused silica and crystalline silicon and was calculated from the final pressure at the crystallization temperature (~700 °C). The effusion temperature T_{eff} is ≈300–350 °C for $T_s < 300$ °C, while for $T_s > 350$ °C, T_{eff} is ≈500 °C. [H] increases monotonically as T_s decreases, as is the case for *a*-Si:H prepared by other methods.[14,19] The observed values of [H] are typically a factor of 2 larger than in HOMOCVD and low-rf-power glow-discharge films, and are of the same order of magnitude as high-rf-power glow-discharge films.[19]

Figure 2 shows the IR spectrum in the range 1900–2200 cm^{-1} for films made at T_s = 100, 200, 300, and 350 °C. Following Lucovsky, Nemanich and Knights,[15] we associate the 2000 cm^{-1} peak with a Si–H stretch mode, while the 2090–2100 cm^{-1} is assigned to the Si–H_2 and $(SiH_2)_n$ stretch modes. These results indicate that most of the H in the LICVD *a*-Si:H is in the Si–H_2 bonding configuration in the film. For T_s = 200 °C, the 2140 cm^{-1} peak characteristic of Si–H_3 (Ref. 15) becomes evident. The 2000 cm^{-1} peak assigned to the SiH bonding configuration is essentially absent for $T_s < 350$ °C. [H] cannot be estimated from the IR spectra since the multiplication factor is known only for a peak centered at 2000 cm^{-1},[15,16] while our films predominantly exhibit the 2090–2140 peak.

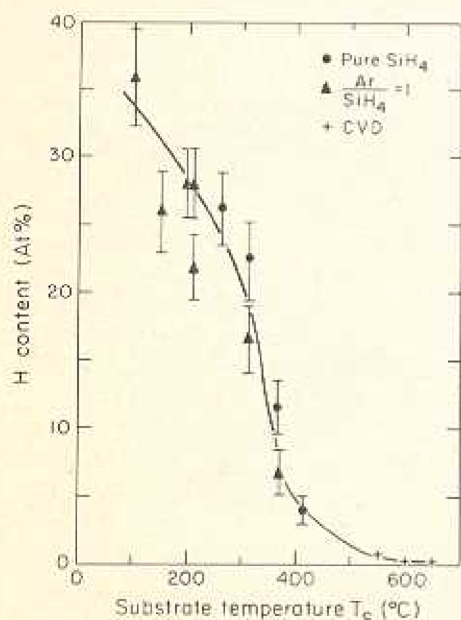

FIG. 1. H concentration [H] as a function of substrate temperature T_s for LICVD and CVD films (from Ref. 18).

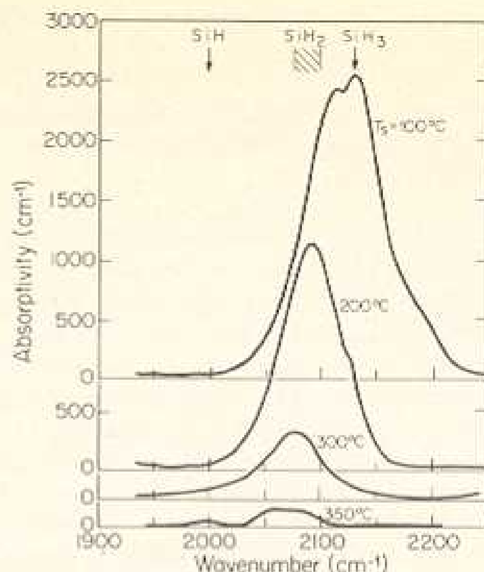

FIG. 2. Infrared spectra in the range 1900–2200 cm^{-1} for films made at T_s = 100, 200, 300, and 350 °C.

Other peaks have been observed in addition to those in the 2000–2100 cm^{-1} range, and their absorptivity as a function of T_s is shown in Fig. 3. Following Lucovsky *et al.*,[15,17] the peak assignments are: 890 cm^{-1}, Si–H_2 and $(SiH_2)_n$ bend scissor; 845 cm^{-1}, polymeric $(SiH_2)_n$ wag; 980 cm^{-1},

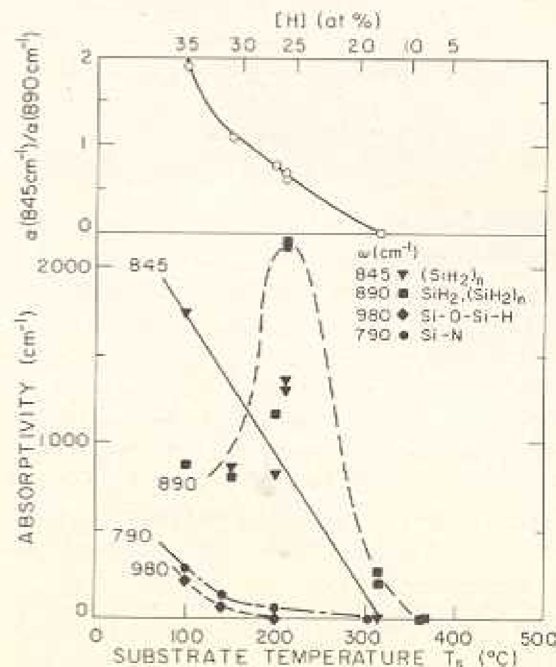

FIG. 3. Absorptivity of various IR peaks and $\alpha(845\ cm^{-1})/\alpha(890\ cm^{-1})$ as a function of substrate temperature T_s.

O stretch in Si–O–Si–H; 790 cm^{-1}, Si–N stretch. Whereas in sputtered,[16] glow-discharge,[17] and HOMOCVD[19] films, the 845 cm^{-1} peak is always smaller than the 890 cm^{-1} peak, in the LICVD films, the ratio $\alpha(845)/\alpha(890)$ can be as high as 2 at $T_s = 100\,°C$, indicating increasing regions of the polymeric structure $(SiH_2)_n$ for T_s below 300 °C. Clearly, most of the H is in the Si–H_2 bonding configuration, and at low T_s ($< 300\,°C$), [H] becomes so large that polymeric chains form. Peaks related to the presence of oxygen and nitrogen increase in strength as T_s decreases below 200 °C. This is probably due to the fact that the film was exposed to air after deposition. Indeed, as pointed out by Schott and Hirschmann,[20] the polymers $(SiH)_n$ and $(SiH_2)_n$ tend to oxidize very quickly when exposed to air. From the results of Lucovsky *et al.*,[17] we estimate that $[O] \simeq 0.8$ at. % at $T_s = 100\,°C$, decreasing to undetectable values ($[O] < 0.05$ at. %) at $T_S \simeq 200\,°C$. The nitrogen content cannot be calculated in this way due to a lack of knowledge about the magnitude of the calibration factor.

III. FILM GROWTH

In the LICVD process, the film growth occurs due to the surface reactions of SiH_2 and possibly higher diradicals (SiH_3SiH, etc.). Following Kampas and Griffith,[21] we assume that the *a*-Si:H surface is fully hydrogenated. Since monoradicals (H, SiH_3, etc.) are absent in the gas,[10,19] the hydrogenated surface of a LICVD film very likely has a much lower concentration of dangling bonds than that of a film deposited by plasma processes. By analogy with the gas-phase chemistry,[22] SiH_2 can insert into any silicon–hydrogen bond ($\equiv$Si–H) with activation energy of approximately 2 kcal/mole to form an activated complex ($\equiv Si\text{–}SiH_3^*$):

$$SiH_2 + \equiv Si\text{–}H \rightarrow \equiv Si\text{–}SiH_3^*. \quad (1)$$

Kampas and Griffith[21] suggested that the activated complex either deactivates at a rate r_1, or eliminates hydrogen at a rate r_2. The latter process is ordinarily followed by a cross-linking step. The ratio r_2/r_1 is then a function of the total H concentration, [H], only and is equal to $(2[H]^{-1} - 3)$.[21]

Figure 4 shows the Arrhenius plot of $r_2/r_1 = 2[H]^{-1} - 3$ as a function of the reciprocal of the substrate temperature T_s for both LICVD and conventional CVD films.[18] Two distinct ranges of behavior can be identified. For $T_s < 300\,°C$, the activation energy is 0.08 eV, essentially the same as the 0.07 eV found in HOMOCVD films.[19] According to Kampas and Griffith,[21] this is just the difference in the activation energies of the H elimination and deactivation processes. For $T_s > 300\,°C$, H evolution occurs and the Arrhenius plot of r_2/r_1 as a function of $1/T_s$ no longer has a simple meaning. In Fig. 4, we also plot log $[H]^{-1}$ as a function of $1/T_s$ for the same data. Again, two regimes are evident. At $T_s < 300\,°C$, an activation energy of 0.05 eV is deduced, similar to the HOMOCVD results.[19] According to Scott, Reimer, and Longeway,[19] this represents those H elimination steps that reach equilibrium quickly compared to the total deposition time. For $T_s > 300\,°C$, evolution occurs with an "apparent" activation energy of 0.68 eV.

The IR results along with the analysis based on previous models [19,21] of our data of [H] as a function of T_s suggest a possible growth mechanism. In the LICVD process, SiH_2 and possibly higher diradicals react on the surface with an activation energy of 0.05–0.08 eV. This is essentially the same as the activation energy of the gas-phase reaction insertion of SiH_2 into any Si–H bond ($\simeq 0.09$ eV).[22] For $T_s < 300\,°C$ ($[H] > 20$ at. %), there is essentially no H_2 evolution and [H] is determined by the surface chemistry involving the competition between the $\text{–}SiH_3^*$ complex deactivation and the H_2 elimination step. In the LICVD process, due to the absence of either any etching by monoradicals or any ion bombardment, the film surface should have a Si–H_2 structure with a very small concentration of dangling bonds. As is evident from the IR results of Fig. 2, this is reflected by predominantly SiH_2 bonding in the films prepared with $T_s < 300\,°C$. As the temperature is lowered, the $\text{–}SiH_3^*$ complex deactivation becomes more predominant over the H_2 elimination step leading to an increase in the concentration of SiH_2 and even to some SiH_3 units. At the lowest temperature, polysilane chains are present in the films, as is clear from Fig. 3. For $T_s > 300\,°C$ ($[H] < 20$ at. %), in addition to the surface chemistry, H_2 evolution during growth controls the hydrogen concentration. Films deposited in this temperature range still have a primarily Si–H_2 structure suggesting that H_2 evolves via the process $SiH_2 \rightarrow Si + H_2$. Only rarely does a single Si–H bond break, a necessary event for the appearance of the Si–H units. However, due to the decrease in the concentration of Si–H_2 units, the 845 cm^{-1} peak disappears above 300 °C, as is evident from Fig. 3. The activation energy of 0.68 eV indicated by the data of Fig. 4 is different from the 1.5 eV usually reported[23] as the activation energy for the H diffusion coefficient D_H, in glow-discharge *a*-Si:H films. This might suggest that a different process, e.g., diffusion of molecular H_2, is the rate-limiting step in LICVD films with a predominantly SiH_2 structure.

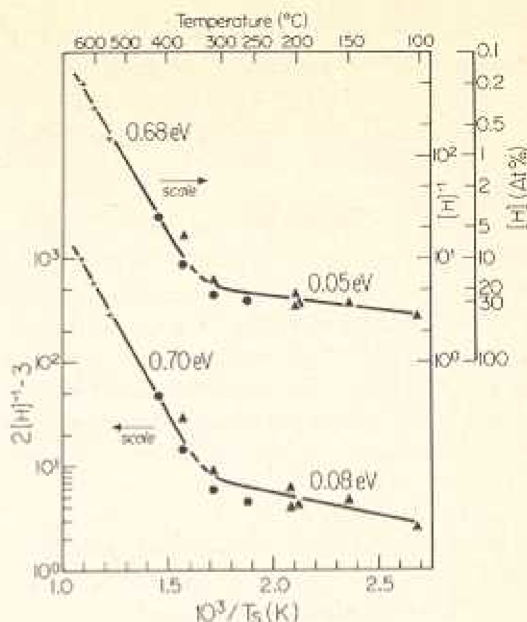

FIG. 4. Arrhenius plot of $2[H]^{-1}$-3 and $[H]^{-1}$ as a function of the reciprocal substrate temperature (+ CVD films; ▲ and ● LICVD, as in Fig. 1).

IV. DEFECTS

The unpaired spin concentration N_s was determined from electron-spin-resonance (ESR) experiments.[24] It is probable that other defects, with paired spins, are also present in the film, but these are difficult to detect.[25] The ESR spectra show the usual line with $g = 2.0055$, indicative of neutral dangling bonds.[24] At low values of microwave power, an additional sharp peak arises at 2.0026. This peak has been attributed by Carlos[26] to the presence of small concentrations of carbon. The concentration of the defects with $g = 2.0026$ is independent of all process parameters and equal to $(6 \pm 2) \times 10^{15}$ cm^{-3}. The concentration of neutral dangling bonds is also independent of laser power and gas pressure, but depends strongly on the substrate temperature T_s.

Figure 5 shows the Arrhenius plot of N_s as a function of $1/T_s$ for both LICVD and conventional CVD films.[27,28] N_s decreases with decreasing T_s, reflecting the increasing hydrogen concentration. All data fit the relationship

$$N_s = (2.7 \times 10^{22}\ \text{cm}^{-3}) \exp(-0.63\ \text{eV}/kT_s), \qquad (2)$$

emphasizing the basic similarity between the LICVD and conventional CVD deposition processes. However, the LICVD process permits films to be deposited at T_s values inaccessible to conventional CVD of SiH_4. The values at the lowest substrate temperatures, $N_s \simeq 8 \times 10^{15}$ cm^{-3}, are of the same order of magnitude as those observed in high-quality films deposited by other techniques,[12,19] but our films do *not* exhibit the minimum N_s observed near $T_s = 300$ °C in both glow-discharge and HOMOCVD films. This difference suggests differences in the processing conditions and gas-phase chemistry. The plasma contains high-energy ions and monoradicals, which could induce defects that do not anneal away at low T_s (<300 °C). HOMOCVD is a thermal process otherwise similar to LICVD, but some monoradicals such as SiH_3 are possibly present because of the hot walls, and those could be the source of the increased N_s at low T_s.

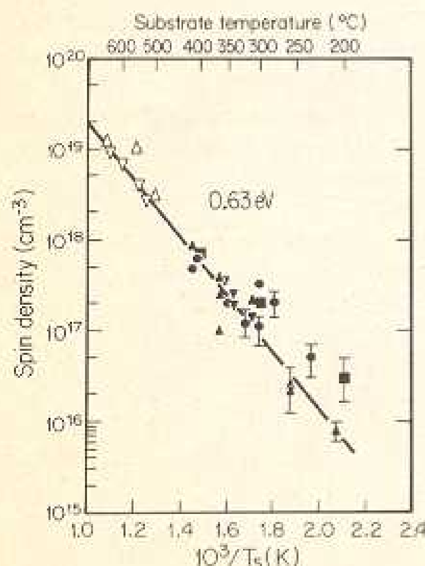

FIG. 5. Spin density N_s vs $1/T_s$ (K^{-1}) for LICVD films: ● 25 W; ▲ 40 W; ▼ 45 W laser powers above the substrate and for normal CVD films; ▽ from Ref. 27; △ from Ref. 28.

The CVD and LICVD results indicate that the concentration of neutral dangling bonds is controlled by a law of mass action at T_s, with a formation energy of 0.63 eV (14.5 kcal/mol). Due to the absence of either ion bombardment of etching by monoradicals, the defect density of films deposited by the LICVD process depends primarily on the steps involving H elimination at the surface and H diffusion to the potential dangling bonds in the growing film. The 0.63 eV activation energy of N_s is not too far from the 0.68 eV activation energy of $[H]^{-1}$ for $T_s > 300$ °C. This suggests that the H evolution process is responsible for both the [H] and the N_s variations in the films. For $T_s > 300$ °C, the N_s [H] product is essentially constant. This can be understood if the H evolution at high temperature, which induces a decrease in [H], also results in an increase in spin density. From the data of Figs. 4 and 5, for $T_s > 300$ °C, we find

$$(N_s [H])^{1/2} \simeq 5 \times 10^{19}\ \text{cm}^{-3}, \qquad (3)$$

where N_s and [H] both have units of cm^{-3}. The microscopic origin of Eq. (3) is not yet well understood, since [H] represents the total H content which probably includes Si–H, Si–H_2, and the molecular H_2 trapped in the microvoids.[30,31] However, N_s should be proportional to the overall strain which monotonically decreases with increasing [H], so that the result is not unreasonable.

An annealing study has been done for four films, deposited at $T_s = 200$, 250, 300, and 400 °C. Figure 6 shows an Arrhenius plot of N_s as a function of the annealing temperature, T_A.[32] Annealing any of these films at $T_A = 250$ °C does not affect N_s. However, upon annealing at 300 °C, N_s changes abruptly and becomes $(2.5 \pm 0.5) \times 10^{17}$ cm^{-3}, independent of T_s, for films processed at $T_s = 300$ °C. This value is the same as when processing the films at $T_s = 350$ °C (see Fig. 5). In this temperature range (300–350 °C), H be-

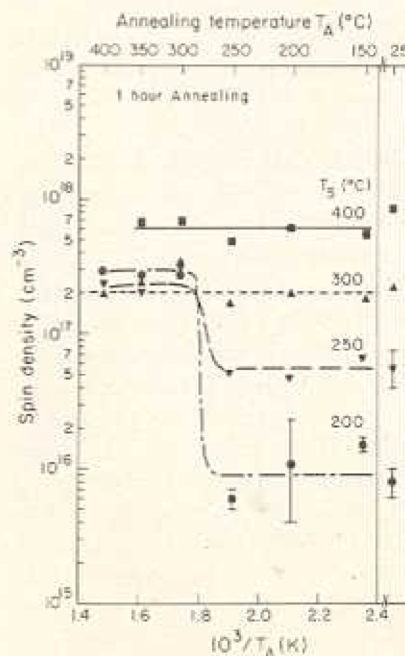

FIG. 6. Spin density as a function of the reciprocal annealing temperature for films processed at substrate temperature $T_s = 200$, 250, 300, and 400 °C (from Ref. 32).

gins to effuse, leaving dangling bonds and other defects behind. Any further annealing up to 400 °C does not change N_s, probably because no further H_2 evolution occurs at these temperatures after the films have been held at 300 °C for 1 h. These results suggest that the relationship between the neutral dangling-bond concentration and the H concentration found in the as-deposited LICVD films also holds after annealing. Note that the absence of annealing effects below the temperature at which hydrogen begins to effuse, e.g., in the $T_s = 200$ °C film below $T_a = 300$ °C, is consistent with the lack of a minimum in Fig. 5.

V. MECHANICAL PROPERTIES

Although most a-Si:H films grown by other processes are ordinarily under compressive stress,[33–36] LICVD films grown on a very thin substrate (0.015 mm) are under tensile stress. Figure 7 shows the stress of film deposited on borosilicate glass (Corning 0211) as a function of T_s, as measured with a He-Ne laser both at $T = T_s$ and at $T = 25$ °C.[37] Also shown is the thermal expansion as deduced from the slope of stress versus measuring temperature.

Films thicker than 2 μm have been grown at $T_s > 350$ °C and at $T_s < 250$ °C; however, films grown at $T_s = 300$ °C peel off the substrate at thickness 0.6–1.0 μm during deposition independent of the thermal stress during the cooling of the sample. These observations are consistent with the fact that the maximum intrinsic stress of 5.1×10^9 dyn/cm^2 is observed in films deposited at $T_s = 300$ °C. We have estimated that the yield stress is 5.6×10^9 dyn/cm^2 which corresponds to a factor of 4.3 larger than the one deduced by Shanks and Ley.[38] The maximum intrinsic stress occurs at the substrate temperature which separates the two growth regimes of Fig. 4. Films made at $T_s < 300$ °C undergo minimum hydrogen evolution during growth, and the top layer which grows under essentially no stress is determined by the

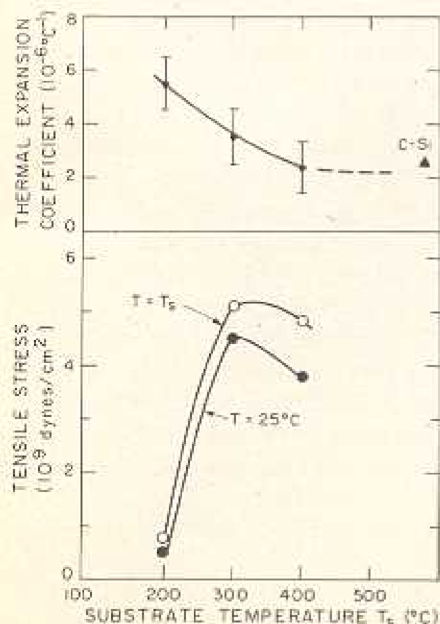

FIG. 7. Thermal expansion coefficient and tensile stress measured at 25 °C and T_s as a function of substrate temperature T_s.

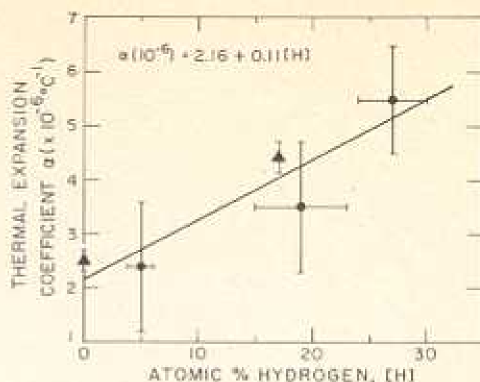

FIG. 8. Thermal expansion coefficient as a function of [H] for LICVD (●). (▲ values are from Ref. 40.)

surface chemistry. Underneath layers are not annealed and the films show minimum internal stress. However, when $T_s = 300$ °C, H diffusion, both towards the surface and the substrate begins to take place causing the internal layers to shrink. Therefore, the films are under tensile stress. Also H_2 diffusion leads to microvoid formations[38,39] introducing additional stress, which can even lead to cracking and blistering when the pressure in the microvoids becomes too large. When the processing temperature is still higher ($T_s > 350$ °C), less hydrogen is present in the film due to both the H_2 elimination at the growing surface and H_2 diffusing out of the film. The annealing process still produces some stress at these substrate temperatures, but smaller than that at $T_s = 300$ °C.

As the film and substrate are cooled from T_s to 25 °C, stress decreases due to the countereffect of thermal stress. Using the thermal-expansion value of 7.4×10^{-6} °C^{-1} for the 0211 Corning glass, we can estimate the thermal expansion α plotted in Fig. 7. Films grown at 400 °C have the same α as crystalline silicon[40] (c-Si). However, as T_s decreases, α increases monotomically, probably due to the incorporation of hydrogen, which changes the local bonding configuration as well as the density. Figure 8 shows α as a function of [H] for LICVD a-Si:H films, c-Si, and glow-discharge a-Si:H films.[40] Qualitatively, the thermal expansion of a solid depends on the anharmonicity of the chemical bonds. Figure 8 suggests that the Si–H bond is more anharmonic than the Si–Si bond, probably due to the difference in electronegativities.

VI. OPTICAL PROPERTIES

The variation of the optical absorption α_v, as a function of photon energy, $E = h\nu$, provides information about the optical gap E_g, defined by the Tauc's expression,[41,42] $(\alpha_v h\nu)^{1/2} = B(h\nu - E_g)$. For LICVD films, E_g is independent of laser power and gas pressure, but increases with decreasing T_s due to the increasing [H] in the films.[43,44] Figure 9 shows E_g as a function of [H] for films made under different conditions. The admixture of the stronger Si–H bonds (the Si–H bond energy of 3.4 eV is about 40% larger than the Si–Si bond energy of 2.4 eV) to the network removes states from the top of the valence band, thereby increasing E_g. Clearly, two distinct regions exist, with a transi-

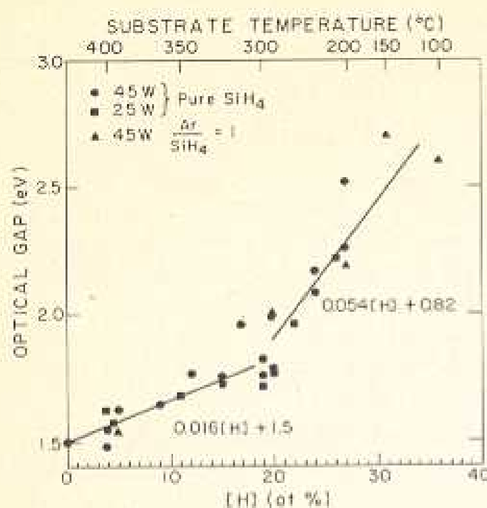

FIG. 9. Optical gap (eV) as a function of [H] concentration for LICVD films processed under various conditions.

tion at $T_s = 300\,^\circ\mathrm{C}$ ($[\mathrm{H}] \simeq 20$ at. %), essentially the same transition temperature found in Fig. 4. For $[\mathrm{H}] < 20$ at. % ($T_s > 300\,^\circ\mathrm{C}$), E_g increases linearly from 1.5 to 1.8 eV. In this temperature range, H_2 diffusion results in the films having a predominantly SiH_2 structure. The observed relationship, $E_g = (0.016[\mathrm{H}] + 1.5)$ eV is the same as the one found by Cody *et. al.*[42] for a films with $[\mathrm{H}] < 30$ at. % and a predominantly SiH structure. This result suggests that E_g depends on only the total H content, independent of the bonding configuration. However, for $[\mathrm{H}] > 20$ at. % ($T_s < 300\,^\circ\mathrm{C}$), E_g increases more rapidly with [H] up to $\simeq 2.7$ eV. In this temperature range, the absence of H_2 evolution leads to a large concentration of SiH_2 units and to the formation of $(SiH_2)_n$ chains. Figure 9 suggests that interaction between Si–H_2 units leads not only to the 845 cm^{-1} IR peak, but also to a larger bonding-antibonding splitting leading to a much larger optical gap. Such a large optical gap is in agreement with a theoretical calculation of the energy band structure of chainlike polysilane alloys.[45]

VII. ELECTRICAL PROPERTIES

The dark conductivity (σ_{dark}) and photoconductivity (σ_{ph}) of LICVD films were measured using a planar sample configuration with a separation of 5×10^{-2} cm between two aluminum contacts. Sandwich configurations gave unreliable results, due to the presence of a non-negligible oxide layer near the surface, as indicated by the IR spectra (see Fig. 3). With the maximum applied field kept at 10^3 V/cm, the lowest measured $\sigma_{\mathrm{dark}} \sim 10^{-13} (\Omega\,\mathrm{cm})^{-1}$. We found that it was essential that the films be deposited on fused silica, due to the high resisivity of the sample, which is in parallel with the substrate.

Figure 10 shows the values of σ_{dark}, σ_{ph}, and the optical gap at 300 K as well as the activation energy (E_{act}) for σ_{dark} estimated from Arrhenius plots in the high-temperature regime for films deposited at several different values of T_s.[46] The photoconductivity was measured using a quartz-halogen lamp ($\simeq 0.5$–$1.1\ \mu$m) with an intensity of about 100

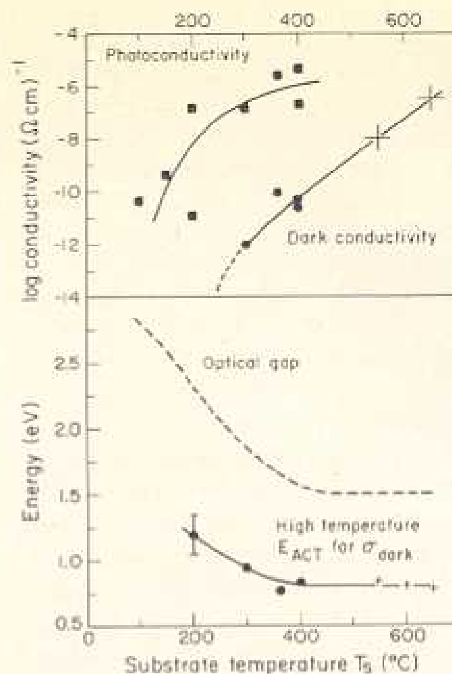

FIG. 10. Room temperature, dark and photoconductivites, optical gap, and high-temperature activation energy for σ_{dark} as a function of substrate temperature. The + are for CVD films (from Ref. 48).

$\mathrm{mW/cm^2}$. E_{act} was calculated in the high-temperature range, because of a small curvature of the Arrhenius plot of σ_{dark} of some films. From a linear extrapolation of the high-temperature measurements, we can estimate that films deposited at $T_s \simeq 200\,^\circ\mathrm{C}$ have σ_{dark} much lower than 10^{-14} $(\Omega\,\mathrm{cm})^{-1}$, possibly as low as $\sim 10^{-17}$ $(\Omega\,\mathrm{cm})^{-1}$ at 300 K. The values for σ_{dark} shown in Fig. 10 are approximately 5 orders of magnitude lower than the ones reported previously,[9] probably due to a systematic experimental error in the previous measurements. Indeed, the σ_{dark} values reported here are for samples deposited on the contacts, while in the previous measurements, contacts were evaporated onto the sample, very likely leading to an additional conduction path through interface states with a higher conductivity.

The dark conductivity of conventional CVD films[47,48] has a constant high-temperature $E_{\mathrm{act}} \simeq 0.8$ eV and a low-temperature ($T < 100\,^\circ\mathrm{C}$) E_{act} that increases as T_s decreases, leading to a relative decrease in the room-temperature value of σ_{dark}. Arrhenius plots of LICVD films show only a small curvature and a high-temperature E_{act} increasing from 0.8 eV to 1.2 ± 0.15 eV as T_s decreases from 400 to 200 °C, leading to a sharp decrease in the room temperature σ_{dark}. Illumination of the films with white light of intensity 100 $\mathrm{mW/cm^2}$ increases the conductivity by about 5 orders of magnitude. The photoconductivity decreases as T_s decreases, due to some extent to the increase in E_g, which decreases the number of absorbed photons. However, the decrease in σ_{ph} by over 4 orders of magnitude as E_g increases from 1.5 to 2.5 eV must be primarily due to the increase in the concentration of recombination centers near midgap. Since the low T_s films have lower concentrations of T_3^0 defects, they must possess larger concentrations of spinless de-

fects in the midgap region.

E_{act} most likely represents the energy difference between the Fermi level E_F and the nearest mobility edge, presumably that of the conduction band. We notice that $E_{act} \simeq E_g/2$, suggesting that E_F is near the middle of the gap for both LICVD and CVD films, independent of the processing conditions. This might be due to a defect band in the middle of the gap pinning E_F, or it could be due to a negative U_{eff} for the dangling bond defect. As the [H] increases by decreasing T_s, the concentration of defects decreases, but more importantly, the gap increases, leading to an increase in E_{act}. Dark and photoconductivites follow the variation of E_{act}, which primarily depends on the H concentration.

Spear and LeComber[49] reported that nonintentionally doped SiH_4 glow-discharge a-Si:H films ($T_s = 350$ °C) are n type, with a room-temperature $\sigma_{dark} \sim 10^{-9} (\Omega\ cm)^{-1}$ and $E_{act} \simeq 0.6$ eV. By incorporating small concentrations of B_2H_6 in the gas, E_F moves towards the middle of the gap. The minimum room-temperature σ_{dark} is $\sim 10^{-12} (\Omega\ cm)^{-1}$ with $E_{act} \simeq 0.8$ eV exactly at midgap. These values correspond to those of our undoped films, which suggest that the two processes lead to different types of defects. This may not be surprising considering how different the film-growth mechanisms and the resulting film structures are in the two processes. HOMOCVD films[13,50] with $T_s \simeq 250$ °C have a room-temperature $\sigma_{dark} \sim 10^{-9}$–$10^{-10} (\Omega\ cm)^{-1}$ with $E_{act} \simeq 0.7$–0.8 eV, only slightly different from our LICVD films. Higher silane CVD films[51] deposited at $440 < T_s < 500$ °C have high-temperature activation energies $E_{act} \simeq 0.7$–0.8 eV with $\sigma_{dark} \simeq 10^{-8}$–$10^{-9} (\Omega\ cm)^{-1}$. These results are consistant with the interpolation that we made between CVD and LICVD data on Fig. 10.

Staebler and Wronski[52] observed that long exposure to light (~ 200 mW/cm^2 for 3 h) decreases both the photoconductivity and dark conductivity of plasma-deposited a-Si:H films. They also noticed that the process is reversible by annealing above $\simeq 150$ °C for about 2 h. This effect has important implications for the stability of semiconductor devices, such as thin-film solar cells.[53] These photoinduced changes were not observed in LICVD films made at $T_s > 300$ °C; however, a decrease in σ_{ph} by a factor of 10–100 has been measured in films processed at $T_s = 200$ °C.[46] (Due to a very low σ_{dark} in films deposited at this T_s, light-induced changes in σ_{dark} were not measurable.) Scott *et al.*[12] failed to observe changes in σ_{dark} with strong exposure to light on HOMOCVD films, and have suggested that plasma-induced defects are responsible for the effect. Ellis *et al.*[51] has also reported a very small Staebler–Wronski effect on higher CVD films. However, Tanielian[54] showed that photoinduced changes in σ_{dark} are almost absent when E_F is midgap or in heavily doped films, but is at a maximum when E_F is near $E_g/4$ and $3E_g/4$. Since LICVD, HOMOCVD, and higher silane CVD films have E_F near $E_g/2$, we might expect that the light-induced effects on σ_{dark} should be minimal. However, the absence of any changes in σ_{dark} usually indicates that the intrinsic defect concentration is sufficiently large to mask light-induced changes, either by reducing the probability of a defect-creating recombination event or because the neutral dangling bond concentration is so large initially that the excess ones created by the light are negligible.[53]

VIII. SUMMARY AND CONCLUSION

All the physical properties of LICVD a-Si:H films appear to be controlled by T_s, and are independent of the laser power and SiH_4 pressure. At least for the small range of growth rates (30–200 Å/min) for the films under investigation, no systematic change in film properties has been observed. The strong variations with T_s suggest that the properties of the films primarily depend on the total H concentration.

LICVD films are superior to those produced by conventional CVD of silane because of the permissibly low substrate temperatures. This results in increased hydrogen concentrations and reduced defect densities. However, LICVD films have higher [H] than plasma films, probably due to the absence of ion bombardment and monoradical etching. The film properties are similar to those made by HOMOCVD in that both have a predominantly Si–H_2 structure with a relatively high optical gap. Nonintentionally doped HOMOCVD and LICVD films are nearly intrinsic, while plasma films are usually somewhat n type, probably due to the defect-related ion bombardment.

LICVD is a cold-wall thermal process in which the thin-film growth is due to the surface reaction of SiH_2 and possibly higher diradicals (SiH_3SiH,...).[10] The gas contains neither highly energetic particles nor monoradicals. These specific conditions result in films with a predominantly Si–H_2 structure. [H] is determined by the surface chemistry for $T_s < 300$ °C ([H] > 20 at. %). At the transition temperature ($T_s = 300$ °C), the films show maximum internal stress due to a relatively large [H], which together with the large value of the H diffusion coefficient leads to both significant annealing and microvoid formation. Due to the absence of both etching by monradicals and ion bombardment, the defect density depends primarily on the steps involving H_2 evolution in the bulk of the growing film. The Arrhenius plots of N_s and $[H]^{-1}$ have the same activation energies (0.63–0.68 eV) for $T_s > 300$ °C. As [H] increases, N_s decreases such that the product N_s [H] is constant.

As expected, incorporation of hydrogen in the films affects the structure and all the properties of the films. The thermal expansion increases linearly with [H], probably due to a greater anharmonicity of the Si–H bonds compared to the Si–Si bonds. The basic unit in LICVD a-Si:H is Si–H_2, whose concentration increases as T_s decreases. For $T_s < 300$ °C, the H_2 evolution becomes very small and the concentration of Si–H_2 units increases sufficiently that chains of $(SiH_2)_n$ form, leading films to have some polymeric regions. The optical gap increases linearly with [H], up to concentrations of 20 at. % hydrogen ($T_s > 300$ °C). However, for $T_s < 300$ °C, ([H] > 20 at. %), the rate of increase of the gap is greater, due to the formation of polymeric regions of $(SiH_2)_n$. In LICVD films, E_F is always near midgap leading to very low values of room-temperature dark conductivity, $\sigma_{dark} \sim 10^{-12} (\Omega\ cm)^{-1}$. Illumination of the films with AM1 light increases σ by factors of $\sim 10^5$, suggesting a relatively low overall defect concentration.

ACKNOWLEDGMENTS

We would like to thank Dr. T. R. Gattuso who carried out much of the pioneering work on the LICVD process. We are also grateful to C. J. Petti, E. Wong, L. V. Atkins, K. Phelan, T. Kramer, E. Pan, A. R. Ralston, P. L. Cheng, M. Hunt, and J. J. Hajjar for their invaluable technical assistance, and to J. D. Casey, A. Jung, C. F. Fuleihan, and B. A. Khan for helpful discussions. The LICVD project has been partially sponsored by the 3M Corporation and the Semiconductor Research Corporation. One of us (M. M.) is grateful for financial aid from the National Research Council of Canada, the Quebec Ministry of Education, and the Standard Oil Co. (SOHIO).

[1]D. Adler and S. R. Ovshinsky, Chemteck **15**, 538 (1985).
[2]P. G. LeComber, W. E. Spear, and A. Ghaith, Electron. Lett. **15**, 179 (1979).
[3]A. J. Snell, W. E. Spear, P. G. LeComber, and K. D. MacKenzie, Appl. Phys. A **26**, 83 (1981).
[4]S. Kishida, Y. Naruke, Y. Uchida, and M. Matsumura, J. Non-Cryst. Solids **59–60**, 1281 (1983).
[5]S. J. Hudgens and A. Johncock, Mater. Res. Soc. Proc. **49**, 379 (1985).
[6]I. Shimizu, S. Oda, K. Saito, H. Tomita, and E. Inoue, J. Phys. (Paris) **42**, C4-1123 (1981).
[7]R. Bilenchi, I. Gianinoni, and M. Musci, J. Appl. Phys. **53**, 6479 (1982).
[8]T. R. Gattuso, M. Meunier, D. Adler, and J. S. Haggerty, *Laser Diagnostics and Photochemical Processing for Semiconductor Devices*, Mater. Res. Soc. Symp. Proc., **17**, 215 (1983).
[9]M. Meunier, T. R. Gattuso, D. Adler, and J. S. Haggerty, Appl. Phys. Lett. **43**, 273 (1983).
[10]M. Meunier, J. H. Flint, J. S. Haggerty, and D. Adler, J. Appl. Phys. **62**, 2812, (1987).
[11]J. C. Knights, R. A. Lujan, M. P. Rosenblum, R. A. Street, D. K. Bieglesen, and J. A. Reimer, Appl. Phys. Lett. **38**, 331 (1981).
[12]B. A. Scott, J. A. Reimer, R. M. Plecenik, E. E. Simonyi, and W. Reuter, Appl. Phys. Lett. **40**, 973 (1982).
[13]B. A. Scott, R. M. Plecenik, and E. E. Simonyi, Appl. Phys. Lett. **39**, 73 (1981).
[14]H. Fritzsche, M. Tanielian, C. C. Tsai, and P. J. Gaczi, J. Appl. Phys. **50**, 3366 (1979).
[15]G. Lucovsky, R. J. Nemanich, and J. C. Knights, Phys. Rev. B **19**, 2064 (1979).
[16]E. C. Freeman and W. Paul, Phys. Rev. B **18**, 4288 (1978).
[17]G. Lucovsky, J. Yang, S. S. Chao, J. E. Tyler, and W. Czubatyi, Phys. Rev. B **28**, 3225 (1983); **28**, 3234 (1983).
[18]P. C. Booth, D. D. Allred, and B. O. Seraphin, J. Non-Cryst. Solids **35–36**, 213 (1980).
[19]B. A. Scott, J. A. Reimer, and P. A. Longeway, J. Appl. Phys. **54**, 6853 (1983).
[20]V. G. Schott and E. Hirschmann, Z. Anorg. Allgen. Chem. **288**, 9 (1956).
[21]F. J. Kampas and R. W. Griffith, Appl. Phys. Lett. **39**, 407 (1981).
[22]P. John and J. H. Purnell, J. Chem. Soc. (Faraday I) **69**, 1455 (1973).
[23]K. Zellama, P. Germain, S. Squelard, B. Bourdon, J. Fontenelle, and R. Danielou, Phys. Rev. B **23**, 6648 (1981).
[24]D. K. Biegelsen, Solar Cells **2**, 421 (1980).
[25]D. Adler, J. Phys. (Paris) **42**, C4-3 (1981).
[26]W. E. Carlos, J. Non-Cryst Solids **66**, 157 (1984).
[27]S. Hasegawa, T. Kasajima, and T. Shimizu, Philos. Mag. B **43**, 149 (1981).
[28]P. Hey and B. O. Seraphin, Solar Energy Mater. **3**, 447 (1980).
[29]H. Fritzche, Solar Energy Mater. **3**, 447 (1980).
[30]W. E. Carlos and P. C. Taylor, Phys. Rev. B **25**, 1435 (1982).
[31]Y. J. Chabal and C. K. N. Patel, Phys. Rev. Lett. **53**, 210 (1984).
[32]E. Wong, S. B. thesis, MIT (1983) (unpublished).
[33]M. Stutzmann (unpublished data).
[34]P. L. Jones, A. S. Korhonen, L. J. Dimmey, F. H. Cocks, and J. T. A. Pollock, Mater. Sci. Eng. **52**, 181 (1982).
[35]K. Ozawa, N. Takagi, and K. Asama, Jpn. J. Appl. Phys. **22**, 767 (1983).
[36]J. P. Harbison, A. J. Williams, and D. V. Lang, J. Appl. Phys. **55**, 946 (1984).
[37]L. V. Atkins, S. B. thesis, MIT (1984) (unpublished).
[38]H. R. Shanks and L. Ley, J. Appl. Phys. **52**, 811 (1981).
[39]A. Jung, Y. Wang, G. Liu, J. Xiang, B. Car, W. Yu, and D. Adler, J. Non-Cryst. Solids **74**, 19 (1985).
[40]A. S. Korhonen, P. L. Jones, and F. H. Cocks, Mater. Sci. Eng. **49**, 127 (1981).
[41]J. Tauc, in *Optical Properties of Solids*, edited by F. Abeles (North-Holland, Amsterdam, 1970), pp. 227–313.
[42]C. D. Cody, C. R. Wronski, B. Abeles, R. B. Stephens, and B. Brooks, Solar Cells **2**, 227 (1980).
[43]M. Meunier, J. H. Flint, D. Adler, and J. S. Haggerty J. Non-Cryst. Solids **59–60**, 699 (1983).
[44]M. Meunier, Ph. D. thesis, MIT (1984) (unpublished).
[45]K. Takeda, N. Matsumoto, and M. Fukuchi, Phys. Rev. B **30**, 5871 (1984).
[46]C. J. Petti, S. B. thesis, MIT (1984) (unpublished).
[47]M. Hirose, J. Phys. (Paris) **42**, C4-705 (1981).
[48]M. Hirose, M. Taniguchi, and Y. Osaka, *Amorphous and Liquid Semiconductors*, edited by W. E. Spear (CICL, University of Edinburgh, 1977), p. 352.
[49]W. E. Spear and P. G. LeComber, Philos. Mag. **33**, 935 (1976).
[50]B. S. Meyerson, B. A. Scott, and D. J. Wolford, J. Appl. Phys. **54**, 1461 (1983).
[51]F. B. Ellis Jr., R. G. Gordon, W. Paul, and B. G. Yacobi, J. Appl. Phys. **55**, 4309 (1984).
[52]D. L. Staebler and C. R. Wronski, J. Appl. Phys. **51**, 3262 (1980).
[53]D. Adler, Solar Cells **9**, 133 (1983).
[54]M. H. Tanielian, Philos. Mag. B **45**, 435 (1982).